FERMILAB-PUB-23-472

Di-Higgs Signatures in Neutral Naturalness

Mario Barela[1] and Rodolfo Capdevilla[2]
[1] *Institute for Theoretical Physics, Sao Paulo State University, Sao Paulo, SP 01140-070, Brazil and*
[2] *Theory Division, Fermi National Accelerator Laboratory, Batavia, IL 60510, USA*

The Higgs boson was the last fundamental piece of the Standard Model to be experimentally confirmed. LHC is embarked in a quest to probe the possibility that this particle provides a portal to new physics. One front of this quest consists in measuring the interactions of the Higgs with itself and with other SM particles to a high precision. In a more exotic front, the LHC is searching for the possibility that a pair of Higgses (HH) is the evidence of a new resonance. Such resonances are predicted in models with extended Higgs sectors, extra dimensions, and in models with exotic bound states. In this paper we show how scalar quirks in Folded Supersymmetry can give rise to HH resonances. We point out a viable sector of the parameter space in which HH is the dominant decay channel for these *squikonium* bound states. We found that future runs of the LHC could discover HH resonances in the range of 0.4 - 1.7 TeV under reasonable assumptions. Furthermore, for a given mass and intensity of the HH signal, the model predicts the branching ratio of the subsequent decay modes of the heavy resonance. Finding the extra decay modes in the predicted pattern can serve as a smoking gun to confirm the model.

1. INTRODUCTION

The current particle physics paradigm is that the Standard Model (SM) is a remarkable and, perhaps, the most successful existing physical theory. However, it is also known to be a low energy description of a much larger construction. This is because of the variety of phenomenological problems that the SM cannot address such as the Baryon asymmetry of the Universe, the mechanism for neutrino mass, flavor, and dark matter, to cite a few. One of the guiding principles in the search for physics beyond the SM has been Naturalness and the Hierarchy Problem (HP). This problem arises because the Higgs mass is quadratically sensitive to new physics scales, and becomes even more intriguing by the lack of evidence of new physics in ever increasing experimental energies. The SM is said unnatural for it does not contain a mechanism to stabilize the Higgs mass.

Solutions to the HP typically feature top partners responsible for cancelling the quadratic contribution to the Higgs mass from top quark loops. This is the case in the Minimal Supersymmetric version of the SM (MSSM). Unfortunately, the fact that the mass of the top partners has been pushed to an uncomfortably high regime by current data gives rise to a smaller leftover tuning referred to as *Little Hierarchy Problem.*

It is the strong interacting quality of the top partners that results in the powerful constraints on their masses. This observation triggered the proposition of *Neutral Naturalness* [1–4] models in which the top partners are neutral with respect to one or various of the subgroups of the SM group. Folded Supersymmetry (F-SUSY) is an example of this type of construction in which top partners are not charged under the SM QCD, but under a *dark* version of it. In this theory the Higgs mass is protected at the one loop level up to characteristic energies of tens of TeV. At this scale and above, it is possible to define an ultraviolet completion of F-SUSY with a fifth dimension compactified over an orbifold [2].

In F-SUSY the dark sector squarks are all heavier than the dark QCD hadronization scale. This causes them to behave as quirks (or squirks for its scalar nature). Pair production of these states results in excited *squirkonium* bound states that relax down to the ground state and decay promptly at collider time scales [5]. Neutral squirkonium, here denoted as $X^0_{\tilde{q}}$, can be produced via $pp \to \gamma/Z \to \tilde{q}\tilde{q}^*$. Typically, these states preferentially decay into dark glueballs independently on the generation of the constituent squarks. Charged squirkonium $X^+_{\tilde{q}}$, produced through $pp \to W \to \tilde{q}'\tilde{q}^*$, of the first and second generation will have a dominant branching ratio (BR) to $W + \gamma$ [5–8]. Now, third-generation charged squirkonium will undergo beta decay in a time scale much faster than relaxation [5], causing the system to decay to $W + X^0_{\tilde{q}}$, where q represents the lighter between stop and sbottom. This final state shows promising results in a variation of the model where $X^0_{\tilde{q}}$ is longed-lived [9].

F-SUSY production of third generation squirks always derives in neutral squirkonium, either by direct production or via beta decay of charged ones. This neutral state then preferentially decays to dark glueballs. One feature of the model is that the 0^{++} dark glueball state can mix with the Higgs boson through loops [10, 11]. This mixing causes the dark glueballs to have a naturally small coupling to SM particles, making them long-lived and a great signal for neutral naturalness models [12–14]. However, glueball production is known to decrease as the mass splitting between the two stop eigenstates increases [13]. This is the regime that we will explore in this paper. We will see how increasing the soft trilinear term $A_t\tilde{t}_L\tilde{t}_R H$ that controls the mixing of the two eigenstops, causes the neutral *stoponium* state $X^0_{\tilde{t}}$ to predominantly decay to a pair of Higgs bosons.

A similar observation was made long ago in the context of the MSSM, where studies of stoponium bound states [15–24] have shown that Higgs decay modes dominate for large stop mixing angles. However, stoponium bound states can only be realized in the MSSM for low stop masses, in a regime excluded by the LHC. Our study brings back the possibility that HH resonances have a connection with the third generation of (s)quarks and Naturalness. Furthermore, we will see how the prediction of the model lies in a range of masses that will be soon explored by the LHC.

This paper is organized as follows: Sec. II gives a brief summary of the model and its unique phenomenological features. Sec. III presents our parametric setting where we define the benchmarks that we will analyze. We also show the theoretical bounds on the parameter space of interest from perturbative unitarity. Sec. IV shows squirkonium production cross section and decay modes. In Sec. V one can find our results for observability of HH resonances at the LHC. Finally, Sec. VI shows our conclusions and discussion.

2. SCALAR QUIRKS IN FOLDED SUSY

In this section we provide a synthesis of F-SUSY concepts that are important for our our analysis. For a complete treatment of the model, including a description of the full supersymmetric ultraviolet completion, we refer the reader to [2]. In F-SUSY, the low energy theory is symmetric under the group $SU(3)_c \times SU(3)_{c'} \times SU(2)_L \times U(1)_Y$. The representation content is that of the MSSM, but with squarks charged not under $SU(3)_c$, but under the *dark* color $SU(3)_{c'}$. The model comprises an additional octet of gluons corresponding to the new color sector.

In order to understand the origin of the strange dynamics this results in, it must be known that the two strong force groups are related to each other in the ultraviolet completion of the theory by a Z_2 symmetry. This ensures that the theory is fully Supersymmetric in the UV. As a consequence, the characteristic scales where confinement dynamics kicks in are close to each other $\Lambda_{c'} \sim \Lambda_c$. In general, a pair-produced particle-antiparticle system will hadronize when the energy density of the flux tube (or string) approaches or exceeds $2m_1$, where m_1 is the lightest quark-like particle in the theory. Differently from QCD, the QCD$'$ particle content does not comprise any species with a mass m smaller than the typical string tension $\Lambda_{c'}$. Because of this, pair creation from the vacuum is suppressed as $\exp(-m_1^2/\Lambda'^2)$ and a produced pair of QCD$'$ particles will form a bound state instead of hadronizing. For this odd behavior, particles with charges of a strong group whose confining scale is much smaller than the lightest charged species mass are called *quirks* [25] – and, in F-SUSY, since they are supersymmetric partners, *squirks*.

At LHC energies and for lightest quirk masses of up to ~ 1 TeV, the squirkonium will typically be produced at a highly excited state. A semiclassical analysis [5] of the strong force bound state shows that the probability of decay only become appreciable after relaxation, *i.e.*, after the excess energy is radiated away through emission of photons or glueballs, and the 2-particle system is left at the lowest lying angular momentum state. The decay of the squirkonium to lightest states will, then, most likely have an s wave contribution. The possibility of detecting the soft signals of the relaxation period have been discussed in [26] where the *anthena* pattern is the smoking gun signature.

Soon after the proposal of F-SUSY, the same authors showed that the $W + \gamma$ final state is the dominant decay mode for first and second generation of squirks. They also show that it is not possible to have a charged squirkonium bound state of the third generation because the heavier constituent will beta-decay in a timescale faster than relaxation [5]. This indicates that only neutral squirkonium of the third generation is possible, a state which preferentially decays to dark glueballs. Now, the third generation is of great important for it is the one intrinsically tied to Naturalness and the hierarchy problem. Our work is motivated by this connection, and we would like to study decay channels of the neutral third-generation squirkonium in F-SUSY beyond those explored in the literature where long-lived glueballs seems to be one of the most interesting signals [12].

We will study the large soft trilinear coupling limit for stoponium, where the decay mode to HH can dominate over glueball formation. Our study only involves interactions of the third generation quarks, squarks and of the Higgs and gauge bosons. We will not make any attempt to fix classical problems of the MSSM like the μ problem or the Higgs mass [27–30]. Our simplified analysis assumes: 1) The lightest stop is the lightest third generation squirk; 2) A neutral stoponium is produced from proton-proton collision at the LHC; 3) This state, initially highly excited, will promptly radiate away energy and angular momentum relaxing down to its ground state; 4) Finally, this ground state squirkonium will decay to a variety of channels with a narrow total width ($\sim 5 - 10\%$). In order to determine if one of these channels can overcome glueball formation, we calculate the complete set of branching ratios and analyze their variation over an interesting sector of parameter space. We now discuss the parameter space of interest in the next section.

3. PARAMETER SPACE AND UNITARITY

The interactions relevant to our study involve third generation squarks, gauge bosons, and the Higgs. These comprise, in principle, the following free parameters $\{\tan\beta,\, \mu,\, A_t,\, A_b,\, m_{\widetilde{Q}_L},\, m_{\tilde{t}_R},\, m_{\tilde{b}_R}\}$, where $\tan\beta$ (or simply t_β) is the ratio v_u/v_d of the vacuum expectation values (vev) of the two Higgses in the model, μ is the parameter of the supersymmetric quadratic scalar term, A_q are the soft trilinear terms of the form $A_q H \widetilde{Q}_L \widetilde{q}_R$, and $m_{\widetilde{Q}_L}, m_{\tilde{t}_R}, m_{\tilde{b}_R}$ are the squark soft masses.

In order to define practical benchmarks, we choose a scenario in which all soft masses are equal *i.e.*, $m_{\widetilde{Q}_L} =$

$m_{\tilde{t}_R} = m_{\tilde{b}_R} \equiv \widetilde{m}_{\rm soft}$ and there is no mixing in the sbottom sector, meaning $m_{\tilde{b}_1} = m_{\tilde{b}_2} = \widetilde{m}_{\rm soft}$. These choices leave us with the following set of free parameters

$$\{t_\beta,\ \mu,\ A_t,\ m_{\tilde{t}_1}\}, \tag{1}$$

where $m_{\tilde{t}_1}$ (or simply $m_{\tilde{t}}$) is the mass of the lightest eigenstop. A given choice of these parameters will determine the mass of the heaviest stop, the soft (and sbottom) mass, and mixing angles.

In our analysis, we will vary the mass of the lightest stop between 200 GeV up to 1 TeV and the soft trilinear parameter from 1 up to a few TeV. It could be argued that a *natural* choice for the other parameters is $(t_\beta, \mu) \sim (1, m_h)$, where m_h is the mass of the SM-like Higgs particle. A *tuned* choice of (t_β, μ) could be defined as one that reflects a hierarchy between the two vev of the model and between μ and the EW scale. Without a rigorous definition of tuning, here we define a set of benchmarks (B1, B2, B3, B4) that go from very small to some degree of tuning:

$$\begin{aligned} &\text{B1:} \quad \mu = 200\,\text{GeV},\ t_\beta = 1 \\ &\text{B2:} \quad \mu = 200\,\text{GeV},\ t_\beta = 10 \\ &\text{B3:} \quad \mu = 1\,\text{TeV},\ t_\beta = 1 \\ &\text{B4:} \quad \mu = 1\,\text{TeV},\ t_\beta = 10. \end{aligned} \tag{2}$$

Perturbative Unitarity

As mentioned above, A_t is the scalar trilinear coupling that controls the $H\tilde{t}_1\tilde{t}_1^*$ vertex strength. Increasing this parameter increases the splitting between the two eigenstops $\tilde{t}_1, \tilde{t}_2$ which, as we will see below, in turn increases the production and HH decay rates of the squirkonium states of interest. However, trilinear terms like A_t cannot be set to arbitrarily large values for these parameters tend to create problems like vacuum instability, tachyonic states, or violation of perturbative unitarity [31, 32]. The first two problems are under control within our reasonable benchmark region, and to analyze the third we now study the partial wave unitarity of the model.

We begin from the partial-wave expansion of the (azimuthally symmetric) scattering amplitude for the scalar $2 \to 2$ process $i \to f \equiv \{a, b\} \to \{c, d\}$, here denoted by $\mathcal{M}_{if}(\theta)$. The j-th coefficient of the expansion is

$$a^j_{if} = \frac{1}{32\pi}\sqrt{\frac{4|\mathbf{p}^i||\mathbf{p}^f|}{2^{\delta_{ab}}2^{\delta_{cd}}}} \int d\theta \mathcal{M}_{if}(\theta) P_j(\theta), \tag{3}$$

where $P_j(\theta)$ are the Legendre polynomials and $\mathbf{p}^i, \mathbf{p}^f$ are the centre of mass three-momentum for the initial and final states respectively. In a multi-process analysis one can construct the matrix $(a^{j=0})_{if}$ taking into account all the initial and final states. To satisfy the unitarity condition, the k-th eigenvalue of this matrix must obey

$$\left|\text{Re}\left(a_0^k\right)\right| \le \frac{1}{2}, \ \ \forall\, k. \tag{4}$$

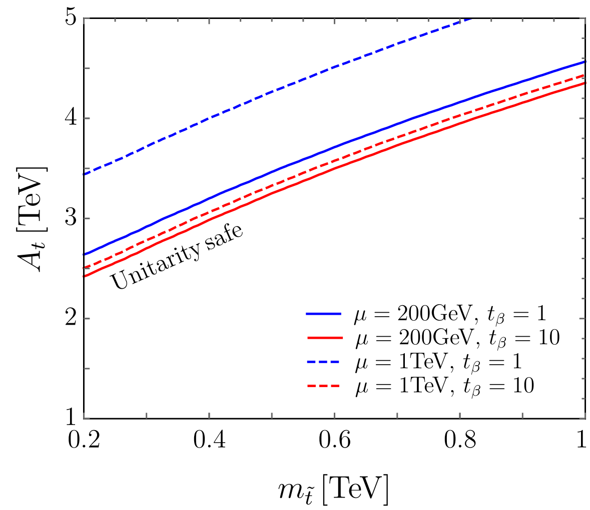

FIG. 1: Maximum A_t allowed by perturbative unitarity as a function of the lightest stop mass.

Note that the constraint above must hold in the entire phase space. To obtain an estimate of the unitarity bounds, we consider the amplitude for the process $\tilde{t}_1\tilde{t}_1^* \to \tilde{t}_1\tilde{t}_1^*$, which include the 4-scalar vertex as well as s- and t-channel exchange of Higgs and dark gluons. The 0-th coefficient is given by[1]

$$a_0 \sim -\frac{1}{24\pi s_\beta^2 v_h^2}\sqrt{1-\frac{4m_{\tilde{t}}^2}{s}}(F_0 + F1 + F_2 + F_3), \tag{5}$$

where

$$\begin{aligned} F_0 =& (3m_t^2 s_{2\theta}^2 + g_s^2 s_\beta^2 c_{2\theta}^2 v_h^2) \\ F_1 =& e^2 s_\beta^2 (9c_\theta^4 + 8s_W^2(2s_\theta^4 - c_\theta^2))/(12c_W^2 s_W^2) \\ F_2 =& \frac{6m_t^2(c_\alpha m_t + s_\theta c_\theta(A_t c_\alpha - s_\alpha \mu))^2}{s - m_h^2} \\ F_3 =& -\frac{s-m_h^2}{s-4m_{\tilde{t}}^2} F_2 \log\left[1 + \frac{s-4m_{\tilde{t}}^2}{m_h^2}\right]. \end{aligned} \tag{6}$$

Here, m_t is the mass of the top quark, v_h is the SM-like Higgs vev, θ is the stop mixing angle, and α/β are the mixing angles of the neutral CP-even/odd components of the two Higgs multiplets in the MSSM [33].

Fig. 1 shows the unitarity bounds corresponding to our four benchmarks defined in Eqs. 2. Below each line the model is unitary safe. We found that for a stop mass of 200 GeV the bound on A_t varies between 2.5 and 3.5 TeV, depending on the benchmark. Note how reducing μ and increasing $\tan\beta$ one may extend the allowed region of parameter space.

[1] These approximate formule ignore terms proportional to EW parameters suppressed by factors of m_Z^2/m_t^2 and $m_Z^2/m_{\tilde{t}_1}^2$. In our analysis and figures no approximations have been considered.

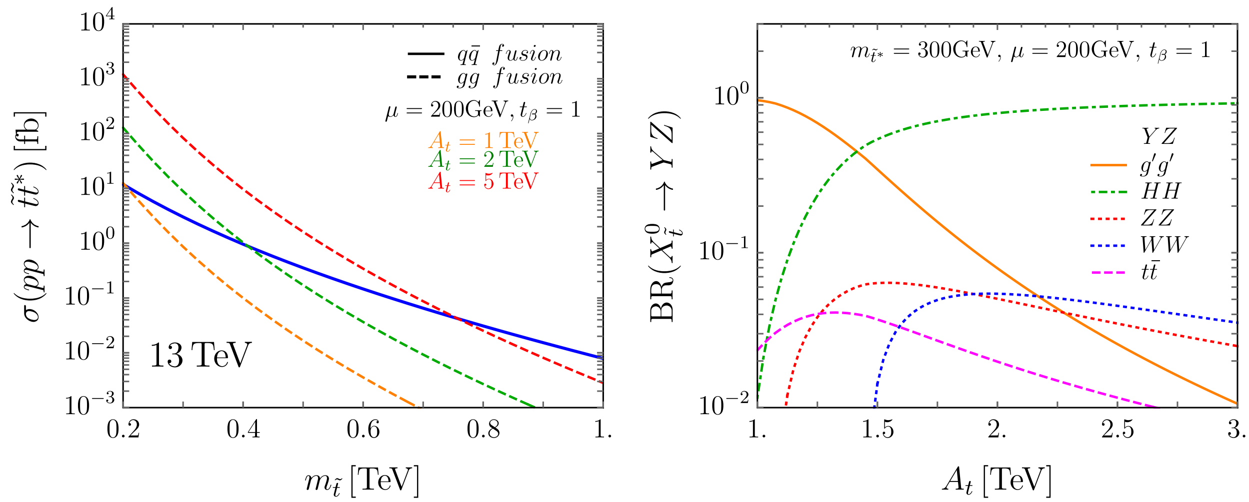

FIG. 2: Left: Production cross section of stoponium at the LHC. For low A_t values, the dominant process is $q\bar{q}$-fusion, whereas gg-fusion dominates for large A_t. Right: Branching Ratios of the lowest lying energy state of the lightest stoponium into the various decay modes as a function of A_t.

For a more refined calculation, one can construct a 5×5 scattering matrix including hh, $\tilde{t}_1\tilde{t}_1^*$, $\tilde{t}_2\tilde{t}_2^*$, $\tilde{b}_1\tilde{b}_1^*$, $\tilde{b}_2\tilde{b}_2^*$ initial and final states. In [31] the authors show how including some of these processes one can extend the unitary bound on A_t up to 4.4 - 5 TeV for stop masses of 100 GeV. We will keep our calculation as a conservative constraint keeping in mind that the full calculation could in principle open a larger region of parameter space.

4. STOPONIUM PRODUCTION AND DECAY

Production

We now discuss the production mechanisms for our squirkonium state of interest at the LHC. In the parameter space that we focus i.e. where the trilinear term A_t is large, the dominant production channels of stoponium $X_{\tilde{t}}^0$ are

$$q\bar{q}\,\text{fusion}: \quad p(q)p(\bar{q}) \to \gamma/Z \to \tilde{t}\tilde{t}^*$$
$$gg\,\text{fusion}: \quad p(g)p(g) \to h \to \tilde{t}\tilde{t}^*.$$

The first process is the usual Drell-Yan, neutral gauge boson mediated, $q\bar{q}$-fusion. The second process is the gg-fusion that involves a triangle top-quark loop and a Higgs in the s-channel. In the limit of large A_t and high center of mass energy, the partonic cross section of the $q\bar{q}$-fusion is given by

$$\hat{\sigma}(q\bar{q} \to \tilde{t}\tilde{t}^*) \approx \frac{\pi\alpha^2}{3\hat{s}}\left(1 - \frac{4m_{\tilde{t}_1}^2}{\hat{s}}\right)^{3/2} f_q(\theta), \qquad (7)$$

where $f_q(\theta) = \alpha_0^q + \alpha_2^q s_\theta^s + \alpha_4^q s_\theta^4$. The dimensionless coefficients α_i^q are given in terms of SM constants and are numerically equal to $\alpha_0^u = 20.3, \alpha_2^u = -32.8, \alpha_4^u = 18.2$, and $\alpha_0^d = 17.6, \alpha_2^d = -39.3, \alpha_4^d = 23.4$. In the same limit of large A_t and $\hat{s}$, the partonic cross section of the gg-fusion process is given by

$$\hat{\sigma}(gg \to \tilde{t}\tilde{t}^*) \approx \frac{6\alpha_s^2 y_t^2 m_t^4}{64^2\pi^3\hat{s}^2 v_h^2}\left(1 - \frac{4m_{\tilde{t}_1}^2}{\hat{s}}\right)^{1/2} g_t(\hat{s}), \qquad (8)$$

$$g_t = \frac{s_{2\theta}^2 A_t^2}{4t_\alpha^2\hat{s}}\left[-4 + \left(1 - \frac{4m_t^2}{\hat{s}}\right)\log^2\left(-\frac{m_t^2}{\hat{s}}\right)\right]^2. \qquad (9)$$

In our calculation we included the effects of u, d, s, c, g partons convoluting the cross section above with the corresponding PDFs for which we used the MSTW2008 set [34].

The cross sections resulting from these channels may be observed in Fig. 2 (left). The $q\bar{q}$-fusion process (solid blue) occurs through gauge interactions and it is independent of A_t. The gg-fusion channel (dashed lines) involves a $H\tilde{t}_1\tilde{t}_1^*$ vertex and it is enhanced with increasing A_t, reason why this channel dominates for an arbitrarily high value of this parameter. Note, for example, that for a mass of $m_{\tilde{t}_1} = 0.4$ TeV the gg-fusion process dominates for $A_t > 2$ TeV.

Decay

In order to calculate the BR of the different decay modes of $X_{\tilde{t}}^0$ we will follow the method in [5]. We calculate the cross section $\sigma(\tilde{t}\tilde{t}^* \to xy)$ for all possible combinations of xy given the interactions of the $X_{\tilde{t}}^0$ state: $g'g', HH, H\gamma, HZ, \gamma\gamma, \gamma Z, ZZ, WW, t\bar{t}$. We then get the annihilation rate $\langle\sigma v\rangle$ taking the limit where the relative velocity v of the $\tilde{t}\tilde{t}^*$ system goes to zero. Finally, the BR for the i-th decay mode is simply $\mathrm{BR}_i = \langle\sigma v\rangle_i / \sum_j \langle\sigma v\rangle_j$.

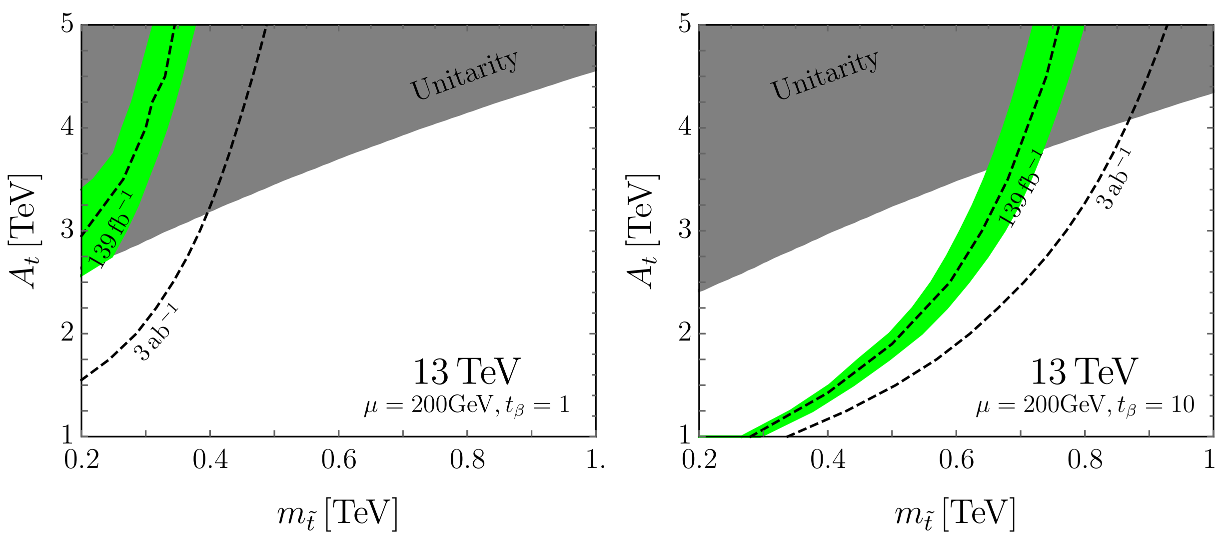

FIG. 3: Exclusion contours on the $(m_{\tilde{t}}, A_t)$ plane for the two *natural* benchmarks. For low t_β the LHC is expected to find low mass resonances in the range of (400, 800) GeV corresponding to $m_{\tilde{t}}$ in the range (200, 400) GeV. As t_β increases, heavier resonances are expected so that for $t_\beta = 10$ a 1.7 TeV resonance is possible.

A priori, one can guess that the dominant decay mode is $g'g'$ due to strong nature of the interaction. Our task is to look for a region of the parameter space where HH can dominate. In the limit $A_t \gg m_{\tilde{t}} \gg m_t, m_h$, the $g'g'$ and HH annihilation rates are equal to

$$\begin{aligned} \langle\sigma v\rangle_{g'g'} \approx& \frac{28\pi\alpha_s^2}{3m_{\tilde{t}}^2}, \\ \langle\sigma v\rangle_{HH} \approx& \frac{3y_t^4 c_\alpha^4 s_{2\theta}^4 A_t^4}{128\pi s_\beta^4 m_{\tilde{t}}^6}. \end{aligned} \tag{10}$$

Here we can observe that for large enough values of A_t, the HH mode is expected to dominate. In agreement with this intuition we can see in Fig. 2 (right) how for large A_t, the $g'g'$ mode (solid orange) is highly suppressed whereas the HH mode (dot-dashed green) BR approaches one.

The effect of increasing the stop mass $m_{\tilde{t}}$ (not shown in the figure) is that all curves in the figure move to the right, meaning that the HH mode starts dominating at higher values of A_t than those shown in the figure. In the relevant parameter space, we found that the modes $H\gamma, HZ, \gamma\gamma, \gamma Z$ were highly suppressed compared to those shown in Fig. 2.

5. Di-Higgs Signals at the LHC

The LHC performs both resonant and non-resonant searches for a pair of Higgs bosons in a variety of final states [35–46]. One of the main motivations of HH searches is to accurately measure the self coupling of the Higgs. The SM has an unfortunate accidental cancellation between the two main diagrams that contribute to HH production, namely, the gluon fusion s-channel Higgs exchange that then splits into two Higgses via self coupling, and the gluon fusion to HH via a top quark box diagram. The total cross section for this process in the SM is about 32.7 fb [47–68]. The main effect of the self coupling is more significant at lower HH invariant masses. Current bounds from non-resonant HH searches at the LHC constrain the trilinear coupling to be within 40% of the SM prediction [69–76].

Now, the fact that HH has a small cross section in the SM opens an opportunity for new physics. In the large invariant mass regime one expects very little irreducible background events. Searches for HH resonances performed in the *bbbb* final states place bounds [43] on masses between 250 GeV and 5 TeV for spin 0 [77] and spin 2 [78] resonances. The bounds on the cross section times HH branching ratio range between a few pb for the lowest masses down to 1 fb for the heaviest mass. [2]

In order to find the reach of the LHC on the parameter space of our model, we calculated the cross section for stoponium production and multiplied by the corresponding BR to HH in the plane $(m_{\tilde{t}}, A_t)$. Our results are presented in Figs. 3 and 4, where we show the exclusion and projections for the different benchmarks defined in Eq. 2. We found that for the *natural* benchmark B1, where $\mu = 200$ and $t_\beta = 1$ (Fig. 3 - left), current LHC data only covers a region of the parameter space that is disfavored by Unitarity. This benchmark predicts that HL-LHC will discover di-Higgs resonances in the range of 400-800 GeV corresponding to stop masses of 200-400 GeV. For the second *natural* benchmark B2, where $\mu = 200$ and $t_\beta = 10$ (Fig. 3 - right), current data exclude

[2] These bounds imply different lower bounds in the HH resonance mass in the context of different models [79–91].

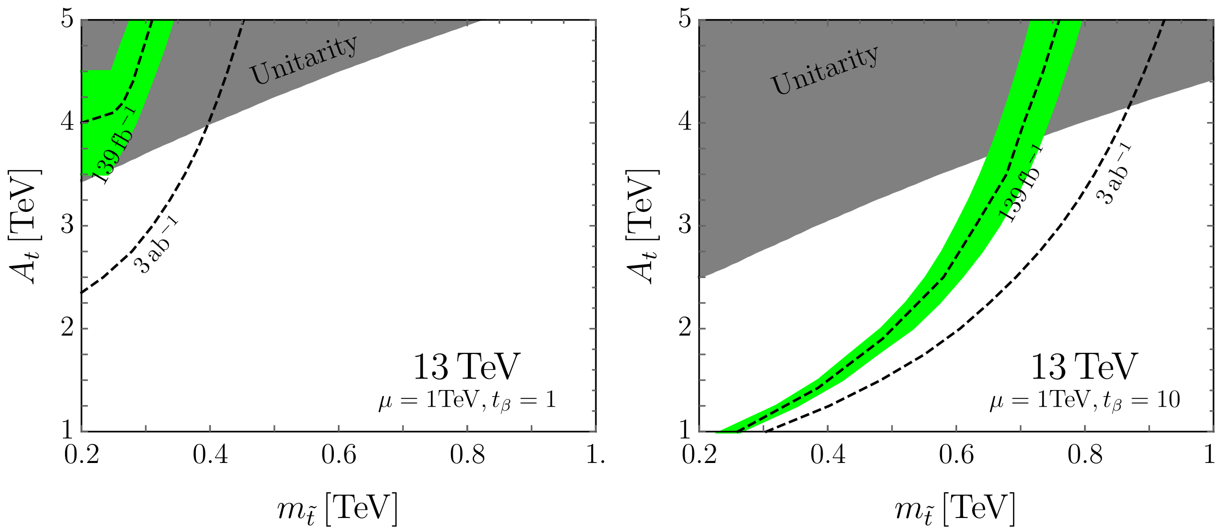

FIG. 4: Similar to Fig. 3 but for the *tunned* benchmarks. The results are similar to those of the *natural* benchmarks because both production and decay of stoponium have a small dependence on μ in the parameter space of interest.

resonances up to 1.4 TeV, corresponding to stop masses of 700 GeV. According to this benchmark, HL-LHC will discover HH resonances up to 1.7 TeV corresponding to stop masses of 850 GeV.

The bottom line of what these results indicate is that the LHC could discover di-Higgs resonances in the range of 400 - 1700 GeV in subsequent runs. This, in a reasonable *natural* region of the parameter space. Furthermore, if LHC finds a HH resonance in this range, according to our analysis, we could be able to infer the value of t_β and A_t within a small window. This in turn will allow us to infer the subsequent decay modes of the resonance according to the right panel of Fig. 2. As we can see in said figure, our resonance will have a significant BR to massive gauge bosons, and if this resonance were to be related to naturalness and the stops, it will also have a significant BR to a pair of top quarks. Finding the same resonance in any of these channels would amount to strong evidence in favour of the model.

The situation for the more *tuned* benchmarks B2 and B3, for which $\mu = 1$ TeV (Fig. 4), is quite similar to what happend for the *natural* benchmarks; future runs of the LHC could discover HH resonances in the range of 400 - 1700 GeV as a function t_β. As discussed in previous sections, our calculations assume stoponium production, fast relaxation, prompt decay, and a narrow width so that our signal efficiency is comparable to those of the LHC searches. Except for the last, all these assumptions were proved to be valid for stoponium in Folded SUSY [5]. If the last assumption were not true and the resonance is broad, our results would not apply, and this represents an opportunity for future work.

Final Remarks

We showed how di-Higgs resonances are predicted in Folded SUSY in the limit of large A_t, the parameter of the trilinear soft SUSY breaking term, in the stop sector. Our results are relevant for subsequent runs at the LHC, where these resonances could be discovered in the range of 400 - 1700 GeV under reasonable assumptions. These values correspond to stop masses between 200 and 850 GeV.

The observation that stoponium bound states preferentially decay to HH has been made in past in the context of the MSSM. However, these bound states can only be conceived in the MSSM for light stops, in a range of masses excluded by LHC searches. Our analysis brings back the possibility that stoponium bound states will produce HH resonances that the LHC will soon discover but this time in the context of F-SUSY. This makes a direct connection between HH resonances, the third generation of (s)quarks, and Naturalness.

Although our analysis focuses on F-SUSY, we argue that the main ingredients of the model that led us to the main results are also present in other models of NN. In general, in NN models the Higgs is the portal between the SM and the *dark* (or *mirror*) sectors. What we showed in this paper is that enhancing the parameter that connects the Higgs with the third generation quirks in the dark sector has two effects: it enhances the production of the corresponding squirkonium state, and it enhances its BR to HH. Once the LHC discovers a HH resonance, a thorough study of its decay modes will serve to unveil the underline theory responsible for said resonance. A pattern like the one in the right panel of Fig. 2 will be a smoking gun pointing at F-SUSY, and it will help us determine some of the model parameters. In a different model of NN the squirkonium bound state will have a different pattern of decays that deserve detailed study in future work.

Acknowledgment

We thank Zackaria Chacko for valuable discussions at the early stage of this work. This manuscript has been authored by Fermi Research Alliance, LLC under Contract No. DE-AC02-07CH11359 with the U.S. Department of Energy, Office of High Energy Physics.

[1] Z. Chacko, H. S. Goh and R. Harnik, "The Twin Higgs: Natural electroweak breaking from mirror symmetry," Phys. Rev. Lett. **96**, 231802 (2006) [arXiv:hep-ph/0506256 [hep-ph]].

[2] G. Burdman, Z. Chacko, H. S. Goh and R. Harnik, "Folded supersymmetry and the LEP paradox," JHEP **02**, 009 (2007) [arXiv:hep-ph/0609152 [hep-ph]].

[3] L. X. Xu, J. H. Yu and S. H. Zhu, "Minimal neutral naturalness model," Phys. Rev. D **101**, no.9, 095014 (2020) [arXiv:1810.01882 [hep-ph]].

[4] B. Batell, M. Low, E. T. Neil and C. B. Verhaaren, "Review of Neutral Naturalness," [arXiv:2203.05531 [hep-ph]].

[5] G. Burdman, Z. Chacko, H. S. Goh, R. Harnik and C. A. Krenke, "The Quirky Collider Signals of Folded Supersymmetry," Phys. Rev. D **78**, 075028 (2008) [arXiv:0805.4667 [hep-ph]].

[6] R. Harnik, G. D. Kribs and A. Martin, "Quirks at the Tevatron and Beyond," Phys. Rev. D **84**, 035029 (2011) [arXiv:1106.2569 [hep-ph]].

[7] G. Burdman, Z. Chacko, R. Harnik, L. de Lima and C. B. Verhaaren, "Colorless Top Partners, a 125 GeV Higgs, and the Limits on Naturalness," Phys. Rev. D **91**, no.5, 055007 (2015) [arXiv:1411.3310 [hep-ph]].

[8] R. M. Capdevilla, R. Harnik and A. Martin, "The radiation valley and exotic resonances in $W\gamma$ production at the LHC," JHEP **03**, 117 (2020) [arXiv:1912.08234 [hep-ph]].

[9] L. Li, E. Salvioni, Y. Tsai and R. Zheng, "Electroweak-Charged Bound States as LHC Probes of Hidden Forces," Phys. Rev. D **97**, no.1, 015010 (2018) [arXiv:1710.06437 [hep-ph]].

[10] J. E. Juknevich, D. Melnikov and M. J. Strassler, "A Pure-Glue Hidden Valley I. States and Decays," JHEP **07**, 055 (2009) [arXiv:0903.0883 [hep-ph]].

[11] J. E. Juknevich, "Pure-glue hidden valleys through the Higgs portal," JHEP **08**, 121 (2010) [arXiv:0911.5616 [hep-ph]].

[12] D. Curtin and C. B. Verhaaren, "Discovering Uncolored Naturalness in Exotic Higgs Decays," JHEP **12**, 072 (2015) [arXiv:1506.06141 [hep-ph]].

[13] Z. Chacko, D. Curtin and C. B. Verhaaren, "A Quirky Probe of Neutral Naturalness," Phys. Rev. D **94**, no.1, 011504 (2016) [arXiv:1512.05782 [hep-ph]].

[14] G. Burdman and G. Lichtenstein, JHEP **08**, 146 (2018) doi:10.1007/JHEP08(2018)146 [arXiv:1807.03801 [hep-ph]].

[15] M. Drees and M. M. Nojiri, "A new signal for scalar top bound state production," Phys. Rev. Lett. **72**, 2324-2327 (1994) [arXiv:hep-ph/9310209 [hep-ph]].

[16] M. Drees and M. M. Nojiri, "Production and decay of scalar stoponium bound states," Phys. Rev. D **49**, 4595-4616 (1994) [arXiv:hep-ph/9312213 [hep-ph]].

[17] S. P. Martin and J. E. Younkin, "Radiative corrections to stoponium annihilation decays," Phys. Rev. D **80**, 035026 (2009) [arXiv:0901.4318 [hep-ph]].

[18] C. Kim, A. Idilbi, T. Mehen and Y. W. Yoon, "Production of Stoponium at the LHC," Phys. Rev. D **89**, no.7, 075010 (2014) [arXiv:1401.1284 [hep-ph]].

[19] N. Kumar and S. P. Martin, "LHC search for di-Higgs decays of stoponium and other scalars in events with two photons and two bottom jets," Phys. Rev. D **90**, no.5, 055007 (2014) [arXiv:1404.0996 [hep-ph]].

[20] B. Batell and S. Jung, "Probing Light Stops with Stoponium," JHEP **07**, 061 (2015) [arXiv:1504.01740 [hep-ph]].

[21] H. Ito, T. Moroi and Y. Takaesu, "Di-Higgs decay of stoponium at a future photon-photon collider," Phys. Rev. D **93**, no.9, 095027 (2016) [arXiv:1602.01231 [hep-ph]].

[22] Z. Kang, "Bound states via Higgs exchanging and heavy resonant di-Higgs," Phys. Lett. B **771**, 313-317 (2017) [arXiv:1606.01531 [hep-ph]].

[23] G. T. Bodwin, H. S. Chung and C. E. M. Wagner, "Higgs-Stoponium Mixing Near the Stop-Antistop Threshold," Phys. Rev. D **95**, no.1, 015013 (2017) [arXiv:1609.04831 [hep-ph]].

[24] G. H. Duan, L. Wu and R. Zheng, "Resonant Higgs pair production as a probe of stop at the LHC," JHEP **09**, 037 (2017) [arXiv:1706.07562 [hep-ph]].

[25] J. Kang and M. A. Luty, "Macroscopic Strings and 'Quirks' at Colliders," JHEP **11**, 065 (2009) [arXiv:0805.4642 [hep-ph]].

[26] R. Harnik and T. Wizansky, "Signals of New Physics in the Underlying Event," Phys. Rev. D **80**, 075015 (2009) [arXiv:0810.3948 [hep-ph]].

[27] P. Batra, A. Delgado, D. E. Kaplan and T. M. P. Tait, "The Higgs mass bound in gauge extensions of the minimal supersymmetric standard model," JHEP **02**, 043 (2004) [arXiv:hep-ph/0309149 [hep-ph]].

[28] P. Draper, G. Lee and C. E. M. Wagner, "Precise estimates of the Higgs mass in heavy supersymmetry," Phys. Rev. D **89**, no.5, 055023 (2014) [arXiv:1312.5743 [hep-ph]].

[29] R. M. Capdevilla, A. Delgado and A. Martin, "Light Stops in a minimal U(1)x extension of the MSSM," Phys. Rev. D **92**, no.11, 115020 (2015) [arXiv:1509.02472 [hep-ph]].

[30] E. A. R. R. and R. Fazio, "High-Precision Calculations of the Higgs Boson Mass," Particles **5**, no.1, 53-73 (2022) [arXiv:2112.15295 [hep-ph]].
.

[31] A. Schuessler and D. Zeppenfeld, "Unitarity constraints on MSSM trilinear couplings," [arXiv:0710.5175 [hep-ph]].

[32] M. D. Goodsell and F. Staub, "Unitarity constraints on general scalar couplings with SARAH," Eur. Phys. J. C **78**, no.8, 649 (2018) [arXiv:1805.07306 [hep-ph]].

[33] S. P. Martin, "A Supersymmetry primer," Adv. Ser. Direct. High Energy Phys. **18**, 1-98 (1998) [arXiv:hep-ph/9709356 [hep-ph]].

[34] A. D. Martin, W. J. Stirling, R. S. Thorne and G. Watt, "Parton distributions for the LHC," Eur. Phys. J. C **63**, 189-285 (2009) [arXiv:0901.0002 [hep-ph]].

[35] A. M. Sirunyan *et al.* [CMS], "Search for Higgs boson pair production in events with two bottom quarks and two tau leptons in proton–proton collisions at $\sqrt{s}$ =13TeV," Phys. Lett. B **778**, 101-127 (2018) [arXiv:1707.02909 [hep-ex]].

[36] M. Aaboud *et al.* [ATLAS], "Search for Higgs boson pair production in the $\gamma\gamma b\bar{b}$ final state with 13 TeV pp collision data collected by the ATLAS experiment," JHEP **11**, 040 (2018) [arXiv:1807.04873 [hep-ex]].

[37] M. Aaboud *et al.* [ATLAS], "Search for resonant and non-resonant Higgs boson pair production in the $b\bar{b}\tau^+\tau^-$ decay channel in pp collisions at $\sqrt{s}$ = 13 TeV with the ATLAS detector," Phys. Rev. Lett. **121**, no.19, 191801 (2018) [erratum: Phys. Rev. Lett. **122**, no.8, 089901 (2019)] [arXiv:1808.00336 [hep-ex]].

[38] A. M. Sirunyan *et al.* [CMS], "Combination of searches for Higgs boson pair production in proton-proton collisions at $\sqrt{s}$ = 13 TeV," Phys. Rev. Lett. **122**, no.12, 121803 (2019) [arXiv:1811.09689 [hep-ex]].

[39] G. Aad *et al.* [ATLAS], "Combination of searches for Higgs boson pairs in pp collisions at $\sqrt{s}$ =13 TeV with the ATLAS detector," Phys. Lett. B **800**, 135103 (2020) [arXiv:1906.02025 [hep-ex]].

[40] B. Di Micco, M. Gouzevitch, J. Mazzitelli, C. Vernieri, J. Alison, K. Androsov, J. Baglio, E. Bagnaschi, S. Banerjee and P. Basler, *et al.* "Higgs boson potential at colliders: Status and perspectives," Rev. Phys. **5**, 100045 (2020) [arXiv:1910.00012 [hep-ph]].

[41] A. Tumasyan *et al.* [CMS], "Search for heavy resonances decaying to a pair of Lorentz-boosted Higgs bosons in final states with leptons and a bottom quark pair at $\sqrt{s}$= 13 TeV," JHEP **05**, 005 (2022) [arXiv:2112.03161 [hep-ex]].

[42] G. Aad *et al.* [ATLAS], "Search for Higgs boson pair production in the two bottom quarks plus two photons final state in pp collisions at $\sqrt{s}$ = 13 TeV with the ATLAS detector," Phys. Rev. D **106**, no.5, 052001 (2022) [arXiv:2112.11876 [hep-ex]].

[43] G. Aad *et al.* [ATLAS], "Search for resonant pair production of Higgs bosons in the $b\bar{b}b\bar{b}$ final state using pp collisions at $\sqrt{s}$ = 13 TeV with the ATLAS detector," Phys. Rev. D **105**, no.9, 092002 (2022) [arXiv:2202.07288 [hep-ex]].

[44] A. Tumasyan *et al.* [CMS], "Search for Higgs boson pairs decaying to WW*WW*, WW*$\tau\tau$, and $\tau\tau\tau\tau$ in proton-proton collisions at $\sqrt{s}$ = 13 TeV," JHEP **07**, 095 (2023) [arXiv:2206.10268 [hep-ex]].

[45] G. Aad *et al.* [ATLAS], "Search for resonant and non-resonant Higgs boson pair production in the $b\bar{b}\tau^+\tau^-$ decay channel using 13 TeV pp collision data from the ATLAS detector," JHEP **07**, 040 (2023) [arXiv:2209.10910 [hep-ex]].

[46] G. Aad *et al.* [ATLAS], "Search for Higgs boson pair production in association with a vector boson in pp collisions at $\sqrt{s}$ = 13 TeV with the ATLAS detector," Eur. Phys. J. C **83**, no.6, 519 (2023) [arXiv:2210.05415 [hep-ex]].

[47] M. Spira, "Effective Multi-Higgs Couplings to Gluons," JHEP **10**, 026 (2016) [arXiv:1607.05548 [hep-ph]].

[48] S. Borowka, N. Greiner, G. Heinrich, S. P. Jones, M. Kerner, J. Schlenk and T. Zirke, "Full top quark mass dependence in Higgs boson pair production at NLO," JHEP **10**, 107 (2016) [arXiv:1608.04798 [hep-ph]].

[49] Q. H. Cao, G. Li, B. Yan, D. M. Zhang and H. Zhang, "Double Higgs production at the 14 TeV LHC and a 100 TeV pp collider," Phys. Rev. D **96**, no.9, 095031 (2017) [arXiv:1611.09336 [hep-ph]].

[50] S. Jones and S. Kuttimalai, "Parton Shower and NLO-Matching uncertainties in Higgs Boson Pair Production," JHEP **02**, 176 (2018) [arXiv:1711.03319 [hep-ph]].

[51] J. Davies, G. Mishima, M. Steinhauser and D. Wellmann, "Double-Higgs boson production in the high-energy limit: planar master integrals," JHEP **03**, 048 (2018) [arXiv:1801.09696 [hep-ph]].

[52] S. P. Jones, M. Kerner and G. Luisoni, "Next-to-Leading-Order QCD Corrections to Higgs Boson Plus Jet Production with Full Top-Quark Mass Dependence," Phys. Rev. Lett. **120**, no.16, 162001 (2018) [erratum: Phys. Rev. Lett. **128**, no.5, 059901 (2022)] [arXiv:1802.00349 [hep-ph]].

[53] M. Grazzini, G. Heinrich, S. Jones, S. Kallweit, M. Kerner, J. M. Lindert and J. Mazzitelli, "Higgs boson pair production at NNLO with top quark mass effects," JHEP **05**, 059 (2018) [arXiv:1803.02463 [hep-ph]].

[54] R. Bonciani, G. Degrassi, P. P. Giardino and R. Gröber, "Analytical Method for Next-to-Leading-Order QCD Corrections to Double-Higgs Production," Phys. Rev. Lett. **121**, no.16, 162003 (2018) [arXiv:1806.11564 [hep-ph]].

[55] D. De Florian and J. Mazzitelli, "Soft gluon resummation for Higgs boson pair production including finite M_t effects," JHEP **08**, 156 (2018) [arXiv:1807.03704 [hep-ph]].

[56] S. Dawson, C. Englert and T. Plehn, "Higgs Physics: It ain't over till it's over," Phys. Rept. **816**, 1-85 (2019) [arXiv:1808.01324 [hep-ph]].

[57] P. Banerjee, S. Borowka, P. K. Dhani, T. Gehrmann and V. Ravindran, "Two-loop massless QCD corrections to the $g + g \to H + H$ four-point amplitude," JHEP **11**, 130 (2018) [arXiv:1809.05388 [hep-ph]].

[58] X. Xu and L. L. Yang, "Towards a new approximation for pair-production and associated-production of the Higgs boson," JHEP **01**, 211 (2019) [arXiv:1810.12002 [hep-ph]].

[59] P. Basler, S. Dawson, C. Englert and M. Mühlleitner, "Showcasing HH production: Benchmarks for the LHC and HL-LHC," Phys. Rev. D **99**, no.5, 055048 (2019) [arXiv:1812.03542 [hep-ph]].

[60] J. Davies, G. Heinrich, S. P. Jones, M. Kerner, G. Mishima, M. Steinhauser and D. Wellmann, "Double Higgs boson production at NLO: combining the exact numerical result and high-energy expansion," JHEP **11**, 024 (2019) [arXiv:1907.06408 [hep-ph]].

[61] J. Davies and M. Steinhauser, "Three-loop form factors for Higgs boson pair production in the large top mass limit," JHEP **10**, 166 (2019) [arXiv:1909.01361 [hep-ph]].

[62] J. Baglio, F. Campanario, S. Glaus, M. Mühlleitner, J. Ronca, M. Spira and J. Streicher, "Higgs-Pair Production via Gluon Fusion at Hadron Colliders: NLO QCD Corrections," JHEP **04**, 181 (2020) [arXiv:2003.03227 [hep-ph]].

[63] J. Amacker, W. Balunas, L. Beresford, D. Bortoletto, J. Frost, C. Issever, J. Liu, J. McKee, A. Micheli and S. Paredes Saenz, *et al.* "Higgs self-coupling measurements using deep learning in the $b\bar{b}b\bar{b}$ final state," JHEP **12**, 115 (2020) [arXiv:2004.04240 [hep-ph]].

[64] J. Baglio, F. Campanario, S. Glaus, M. Mühlleitner, J. Ronca and M. Spira, "$gg \to HH$: Combined uncertainties," Phys. Rev. D **103**, no.5, 056002 (2021) [arXiv:2008.11626 [hep-ph]].

[65] G. Wang, Y. Wang, X. Xu, Y. Xu and L. L. Yang, "Efficient computation of two-loop amplitudes for Higgs boson pair production," Phys. Rev. D **104**, no.5, L051901 (2021) [arXiv:2010.15649 [hep-ph]].

[66] D. de Florian, I. Fabre, G. Heinrich, J. Mazzitelli and L. Scyboz, "Anomalous couplings in Higgs-boson pair production at approximate NNLO QCD," JHEP **09**, 161 (2021) [arXiv:2106.14050 [hep-ph]].

[67] L. Huang, S. b. Kang, J. H. Kim, K. Kong and J. S. Pi, "Portraying double Higgs at the Large Hadron Collider II," JHEP **08**, 114 (2022) [arXiv:2203.11951 [hep-ph]].

[68] S. Alioli, G. Billis, A. Broggio, A. Gavardi, S. Kallweit, M. A. Lim, G. Marinelli, R. Nagar and D. Napoletano, "Double Higgs production at NNLO interfaced to parton showers in GENEVA," JHEP **06**, 205 (2023) [arXiv:2212.10489 [hep-ph]].

[69] J. H. Kim, Y. Sakaki and M. Son, "Combined analysis of double Higgs production via gluon fusion at the HL-LHC in the effective field theory approach," Phys. Rev. D **98**, no.1, 015016 (2018) [arXiv:1801.06093 [hep-ph]].

[70] D. Gonçalves, T. Han, F. Kling, T. Plehn and M. Takeuchi, "Higgs boson pair production at future hadron colliders: From kinematics to dynamics," Phys. Rev. D **97**, no.11, 113004 (2018) [arXiv:1802.04319 [hep-ph]].

[71] G. Heinrich, S. P. Jones, M. Kerner, G. Luisoni and L. Scyboz, "Probing the trilinear Higgs boson coupling in di-Higgs production at NLO QCD including parton shower effects," JHEP **06**, 066 (2019) [arXiv:1903.08137 [hep-ph]].

[72] P. Agrawal, D. Saha, L. X. Xu, J. H. Yu and C. P. Yuan, "Determining the shape of the Higgs potential at future colliders," Phys. Rev. D **101**, no.7, 075023 (2020) [arXiv:1907.02078 [hep-ph]].

[73] G. Heinrich, S. Jones, M. Kerner, G. Luisoni and L. Scyboz, "Trilinear Higgs boson coupling variations for di-Higgs production with full NLO QCD predictions in Powheg," J. Phys. Conf. Ser. **1525**, no.1, 012009 (2020)

[74] G. Aad *et al.* [ATLAS], "Constraints on the Higgs boson self-coupling from single- and double-Higgs production with the ATLAS detector using pp collisions at s=13 TeV," Phys. Lett. B **843**, 137745 (2023) [arXiv:2211.01216 [hep-ex]].

[75] F. Arco, S. Heinemeyer, M. Mühlleitner and K. Radchenko, "Sensitivity to Triple Higgs Couplings via Di-Higgs Production in the 2HDM at the (HL-)LHC," [arXiv:2212.11242 [hep-ph]].

[76] L. Alasfar, L. Cadamuro, C. Dimitriadi, A. Ferrari, R. Gröber, G. Heinrich, T. I. Carlson, J. Lang, S. Ördek and L. P. Sánchez, *et al.* "Effective Field Theory descriptions of Higgs boson pair production," [arXiv:2304.01968 [hep-ph]].

[77] I. M. Lewis and M. Sullivan, "Benchmarks for Double Higgs Production in the Singlet Extended Standard Model at the LHC," Phys. Rev. D **96**, no.3, 035037 (2017) [arXiv:1701.08774 [hep-ph]].

[78] A. Carvalho, "Gravity particles from Warped Extra Dimensions, predictions for LHC," [arXiv:1404.0102 [hep-ph]].

[79] H. L. Li, M. Ramsey-Musolf and S. Willocq, "Probing a scalar singlet-catalyzed electroweak phase transition with resonant di-Higgs boson production in the $4b$ channel," Phys. Rev. D **100**, no.7, 075035 (2019) [arXiv:1906.05289 [hep-ph]].

[80] C. R. Chen, Y. X. Lin, V. Tran and T. C. Yuan, "Pair production of Higgs bosons at the LHC in gauged 2HDM," Phys. Rev. D **99**, no.7, 075027 (2019) [arXiv:1810.04837 [hep-ph]].

[81] K. Cheung, A. Jueid, C. T. Lu, J. Song and Y. W. Yoon, "Disentangling new physics effects on nonresonant Higgs boson pair production from gluon fusion," Phys. Rev. D **103**, no.1, 015019 (2021) [arXiv:2003.11043 [hep-ph]].

[82] H. Abouabid, A. Arhrib, D. Azevedo, J. E. Falaki, P. M. Ferreira, M. Mühlleitner and R. Santos, "Benchmarking di-Higgs production in various extended Higgs sector models," JHEP **09**, 011 (2022) [arXiv:2112.12515 [hep-ph]].

[83] Anisha, L. Biermann, C. Englert and M. Mühlleitner, "Two Higgs doublets, effective interactions and a strong first-order electroweak phase transition," JHEP **08**, 091 (2022) [arXiv:2204.06966 [hep-ph]].

[84] Y. L. Chung, K. Cheung and S. C. Hsu, "Sensitivity of two-Higgs-doublet models on Higgs-pair production via bbbb final state," Phys. Rev. D **106**, no.9, 095015 (2022) [arXiv:2207.09602 [hep-ph]].

[85] S. Iguro, T. Kitahara, Y. Omura and H. Zhang, "Chasing the two-Higgs doublet model in the di-Higgs boson production," Phys. Rev. D **107**, no.7, 075017 (2023) [arXiv:2211.00011 [hep-ph]].

[86] J. Baglio, F. Campanario, S. Glaus, M. Mühlleitner, J. Ronca and M. Spira, "Full NLO QCD predictions for Higgs-pair production in the 2-Higgs-Doublet Model," [arXiv:2303.05409 [hep-ph]].

[87] C. Englert and J. Jaeckel, "Probing the Symmetric Higgs Portal with Di-Higgs Boson Production," Phys. Rev. D **100**, no.9, 095017 (2019) [arXiv:1908.10615 [hep-ph]].

[88] L. Alasfar, R. Corral Lopez and R. Gröber, "Probing Higgs couplings to light quarks via Higgs pair production," JHEP **11**, 088 (2019) [arXiv:1909.05279 [hep-ph]].

[89] S. Moretti, L. Panizzi, J. Sjölin and H. Waltari, "Deconstructing squark contributions to di-Higgs production at the LHC," Phys. Rev. D **107**, no.11, 115010 (2023) [arXiv:2302.03401 [hep-ph]].

[90] P. Gabriel, M. Mühlleitner, D. Neacsu and R. Santos, "Dark Coloured Scalars Impact on Single and Di-Higgs Production at the LHC," [arXiv:2308.07023 [hep-ph]].

[91] S. Banerjee, B. Batell and M. Spannowsky, "Invisible decays in Higgs boson pair production," Phys. Rev. D **95**, no.3, 035009 (2017) [arXiv:1608.08601 [hep-ph]].